3. 書籍

著者氏名	論文タイトル名	書籍全体の編集者名	書籍名	出版社名	出版地	出版年	ページ
玉城信治、泉並木	TypeⅢインターフェロン	榎本信幸、竹原徹郎、持田智	C型肝炎の診療を極める	文光堂	東京	2014	171-175
黒崎雅之、泉並木	データマイニングによる予後・治療反応予測	榎本信幸、竹原徹郎、持田智	C型肝炎の診療を極める	文光堂	東京	2014	121-129
黒崎雅之、泉並木	肝発癌リスクの評価	田中榮司、竹原徹郎、持田智	B型肝炎の診療を極める	文光堂	東京	2014	152-159

Ⅳ．研究成果の刊行物・別刷

Hepatology Research

Hepatology Research 2014; 44: 920–934 doi: 10.1111/hepr.12199

Original Article

Augmented hepatic Toll-like receptors by fatty acids trigger the pro-inflammatory state of non-alcoholic fatty liver disease in mice

Koji Sawada,[1] Takaaki Ohtake,[1] Takumu Hasebe,[1] Masami Abe,[1] Hiroki Tanaka,[2] Katsuya Ikuta,[1] Yasuaki Suzuki,[4] Mikihiro Fujiya,[1] Chitomi Hasebe[3] and Yutaka Kohgo[1]

[1]Department of Medicine, Division of Gastroenterology and Hematology/Oncology, [2]Department of Gastrointestinal Immunology and Regenerative Medicine, Asahikawa Medical University, [3]Department of Gastroentelorogy, Asahikawa Red Cross Hospital, Asahikawa, and [4]Department of Gastroenterology, Nayoro City General Hospital, Nayoro, Japan

Aim: There is considerable evidence that intestinal microbiota are involved in the development of metabolic syndromes and, consequently, with the development of non-alcoholic fatty liver disease (NAFLD). Toll-like receptors (TLRs) are essential for the recognition of microbiota. However, the induction mechanism of TLR signals through the gut-liver axis for triggering the development of non-alcoholic steatohepatitis (NASH) or NAFLD remains unclear. In this study, we investigated the role of palmitic acid (PA) in triggering the development of a pro-inflammatory state of NAFLD.

Methods: Non-alcoholic fatty liver disease was induced in mice fed a high fat diet (HFD). The mice were killed and the expression of TLRs, tumor necrosis factor (TNF), interleukin (IL)-1β, and phospho-interleukin-1 receptor-associated kinase 1 in the liver and small intestine were assessed. In addition, primary hepatocytes and Kupffer cells were treated with PA, and the direct effects of PA on TLRs induction by these cells were evaluated.

Results: The expression of inflammatory cytokines such as TNF, IL-1β, and TLR-2, -4, -5, and -9 was increased in the liver, but decreased in the small intestine of HFD-fed mice *in vivo*. In addition, the expression of TLRs in primary hepatocytes and Kupffer cells was increased by treatment with PA.

Conclusion: In the development of the pro-inflammatory state of NAFLD, PA triggers the expression of TLRs, which contribute to the induction of inflammatory cytokines through TLR signals by intestinal microbiota.

Key words: fatty acids, gut-liver axis, non-alcoholic fatty liver disease, pro-inflammatory state, Toll-like receptor

INTRODUCTION

NON-ALCOHOLIC FATTY LIVER disease (NAFLD) is a form of steatosis with or without inflammation of the liver, and it is not related to excessive alcohol intake. NAFLD includes both simple steatosis and non-alcoholic steatohepatitis (NASH), the latter developing further into cirrhosis and hepatocellular carcinoma.[1] NAFLD is one of the most common liver diseases worldwide and is considered to be related to obesity, insulin resistance, and metabolic syndrome.[2]

A two-hit theory has been proposed to explain the pathogenesis of NASH.[3] First, simple steatosis is induced by obesity and insulin resistance. Second, NASH develops by several hits, including adipocytokines, iron, and bacterial endotoxins/lipopolysaccharide (LPS) derived from gram-negative bacteria.[4–6]

Toll-like receptors (TLRs) recognize pathogen- and endogenous damage-associated molecular patterns and activate nuclear factor-κB (NF-κB), which induces pro-inflammatory cytokines/chemokines and type 1 interferon through phosphorylation of interleukin-1 receptor-associated kinase 1 (IRAK1) and IRAK4.[7] Therefore, TLRs may play important roles in the activation of innate immunity. Among TLRs, TLR2, TLR4, TLR5, and

Correspondence: Dr Takaaki Ohtake, Department of Medicine, Division of Gastroenterology and Hematology/Oncology, Asahikawa Medical University, 2-1 Midorigaoka Higashi, Asahikawa 078-8510, Japan. Email: totake@asahikawa-med.ac.jp

Received 30 January 2013; revision 18 June 2013; accepted 1 July 2013.

TLR9 were identified as bacterial recognition receptors capable of recognizing lipopeptide, LPS, flagellin, and CpG-DNA, respectively.[8] Recently it was reported that TLR signal pathways, the ligands of which are bacterial components, play an important role in the pathogenesis of alcoholic liver disease and NASH.[9] In particular, the association between TLR4 signal pathways and the development of NASH was investigated.[6,10,11] More recently, Miura *et al.* reported decreased levels of steatohepatitis and liver fibrosis in TLR9 knockout mice compared with those in wild-type mice in a choline-deficient amino acid-defined (CDAA) diet-induced NASH model.[12] In contrast, in TLR2-deficient mice fed a methionine- and choline-deficient (MCD) diet, an increased level of liver injury was noted, suggesting a potential protective role of TLR2 in fatty liver.[6]

An increasing proportion of the general population suffers from obesity, which is an emerging global problem along with its related disorders such as metabolic syndrome. Much recent evidence shows that microbiota are associated with these conditions.[13–19] In the intestine, TLRs are typically expressed in the epithelial cells and are involved in the production of immunoglobulin A (IgA), maintenance of tight junctions, proliferation of epithelial cells, and expression of antimicrobial peptides.[20] TLR5, which specifically recognizes flagellin, is involved in promoting the pathophysiology of inflammatory bowel disease.[21] While the above reports suggest that intestinal TLRs play an important role in innate immunity of the gut, the association between their role in the small intestine and that in the development of NASH remains unclear.

The present study was based on hypernutrition and obesity and evaluated the significance of TLRs and their signaling in the liver and small intestine using a high-fat diet (HFD)-induced NAFLD mouse model. In addition, a gut-sterilized mouse model treated with antibiotics was used to confirm whether there is an association between intestinal microbiota and TLR expression.

METHODS

Animal studies

IN THE HFD group, 8-week-old male C57BL/6J mice (Charles River Japan, Tokyo, Japan) were fed a HFD containing 60% triglycerides with oleic acid (OA), palmitic acid (PA), and stearic acid (Table 1) (F2HFD2; Oriental Yeast Company, Tokyo, Japan). Control mice were fed a diet containing 5% triglycerides (MF; Oriental Yeast Company). All mice were maintained under controlled conditions (22°C; humidity, 50–60%, 12-h light/dark cycle) with food and water *ad libitum*. Mice from both groups were killed at 4, 8, and 16 weeks for blood and tissue collection. These animals were fasted for 10-h before blood and tissue collection. After each mouse was anesthetized with diethyl ether and weighed, blood was collected by a cardiac puncture and subsequently assayed for biochemical parameters. The liver and small intestine were dissected, weighed, and frozen in liquid nitrogen. These samples were used later for histological and polymerase chain reaction (PCR) analysis. All experiments were performed in accordance with the rules and guidelines of the Animal Experiment Committee of Asahikawa Medical University.

Table 1 Composition of fatty acids in control diet and high fat diet

	Control diet (%)	High fat diet (%)
Oleic acid	No detect	30
Palmitic acid	No detect	25
Stearic acid	0.22	16
Palmitoleic acid	0.05	2.0
Myristic acid	0.03	1.5

Isolation and primary culture of hepatocytes and Kupffer cells

Mouse hepatocytes and Kupffer cells were isolated using a modified collagenase perfusion method.[22] Briefly, the liver was perfused via the portal vein with Ca^{2+} and Mg^{2+} free Hank's balanced salt solution (HBSS(−)) at 39°C for 5 min at 10 mL/min, followed by HBSS(+) for 5 min at 10 mL/min supplemented with 0.05% collagenase (Wako, Tokyo, Japan). The liver was then removed, fragmented and vortexed for a few seconds. After filtration with mesh, the cell suspension was centrifuged at 500 rpm for 1 min. The cells in the pellet were minced twice and used as primary hepatocytes for culture in William's E medium with epidermal growth factor (5 μg), insulin (5 mg), L-glutamine, penicillin, streptomycin, and 10% fetal bovine serum (FBS). The supernatant was centrifuged at 500 rpm for 1 min at three to four times to remove any remaining hepatocytes. The supernatant was then minced twice and cultured in Dulbecco's modified Eagle's medium with penicillin, streptomycin, and 10% FBS. After 60 min, adhesion cells were used as Kupffer cells.

PA treatment

Isolated hepatocytes and Kupffer cells were treated with PA. PA complexed with 1% bovine serum albumin

(BSA) was added to the medium to attain final concentrations of 10 μM and 100 μM over 24 h.

Fat droplet evaluation

4,4-difluoro-1,3,5,7,8-pentamethyl-4-bora-3a,4a-diazas-indacene (BODIPY 493/503, Invitrogen, Carlsbad, CA, USA) was added as a lipid probe overnight to the culture medium and fluorescent images were observed.

Biochemical analyses

Serum alanine aminotransferase (ALT) and free fatty acids were measured using the Automatic Analyzer 7180 (Hitachi High-Technologies Corporation, Tokyo, Japan).

Histopathological evaluation

Samples of remaining liver tissue were fixed in 10% formalin buffer, embedded in paraffin, sectioned, and stained with hematoxylin and eosin (H&E).

RNA isolation and first strand complementary DNA synthesis

Total RNA was isolated from the liver, small intestine, primary hepatocytes, and Kupffer cells using QIAGEN RNeasy Mini Kit (QIAGEN, Hilden, Germany). RNA was reverse-transcribed by RETROscript using Random decamers (Ambion, Austin, TX, USA). Detailed methods were performed according to the manufacturers' instructions.

Primer pairs of TLR-related molecules

Mouse 18srRNA was used as an endogenous amplification control. The use of this universally expressed housekeeping gene allows for correction of variations in the efficiency of RNA extraction and reverse transcription. TaqMan assays were used for specific primer and probe sets on TLR2, TLR4, TLR5, TLR9, tumor necrosis factor (TNF), interleukin (IL)-1β, and 18srRNA (Applied Biosystems, Foster City, CA, USA).

Quantitative real-time PCR

The expression of TLR2, TLR4, TLR5, TLR9, IL-1β, and TNF in mouse liver, small intestine, primary hepatocytes, and Kupffer cells was evaluated by quantitative real-time PCR (qPCR) (7300 Real-time PCR system; Applied Biosystems). In this method, all reactions were run in 96-well plates with a total volume of 20 μL. The reaction mixture consisted of 10 μL TaqMan Universal PCR Master mix, 1 μL 18srRNA, 1 μL primer, 5 μL RNAase free water, and 3 μL complementary DNA. The PCR reaction involved the following steps: (i) 50°C for 2 min to prevent carryover of DNA, (ii) 95°C for 10 min to activate polymerase, and (iii) 40 cycles each of 95°C for 15 s, 60°C for 15 s, and 72°C for 45 s. qPCR data were analyzed by the comparative CT method.

Immunohistochemistry/ immunocytochemistry

Immunohistochemistry using F4/80 as a macrophage marker was performed on cryostatically sectioned liver and staining was performed by immunofluorescence. The sections were fixed in 2% paraformaldehyde for 10 min and washed three times with PBS for 5 min. Furthermore, sections for F4/80 were blocked with 3% BSA/PBS for 1 h at room temperature, followed by incubation with monoclonal antibody against F4/80 (Abcam, Cambridge, MA, USA) 1:100 diluted in 3% BSA/PBS for 1 h at room temperature. After washing, F4/80 slides were incubated with 1:200 diluted Alexa Fluor 488 goat anti-rat IgG (Invitrogen) for 1 h at room temperature and washed.

Immunocytochemical staining was also performed using the immunofluorescence method. After the chamber slides in which primary Kupffer cells had been cultured were washed twice with PBS for 5 min, primary Kupffer cells were fixed in 2% paraformaldehyde for 20 min and washed twice with PBS for 5 min. Primary Kupffer cells were then incubated with 0.1% Triton X-100 in PBS for 2 min to permeabilize the membranes and washed twice with PBS. The slides for phospho-interleukin-1 receptor-associated kinase1 (pIRAK1; Abcam) were blocked with 3% BSA/PBS for 1 h at room temperature, followed by incubation with monoclonal antibody against pIRAK1 diluted 1:500 in 3% BSA/PBS for 1 h at room temperature. After washing, the slides were incubated with 1:500 diluted Alexa Fluor 594 goat anti-rat IgG (Invitrogen) for 1 h at room temperature and washed.

Western blotting analysis

Protein expression of pIRAK1, the key mediator in the TLR signaling pathway,[23] in the liver (30 μg), small intestine (30 μg) was studied by Western blot analysis. Protein concentrations were measured by the Bradford method using the Pierce BCA Protein Assay kit (Thermo Scientific, Rockford, IL, USA) according to the manufacturer's instructions. Separation of 30 μg of protein was then performed by 12% Mini PROTEAN TGX Precast Gels (Bio-Rad, Hercules, CA, USA). After electrophoresis, proteins were transferred to nitrocellulose membranes (Amersham Life Science Piscataway, NJ, USA),

blocked in 5% skim milk, and 0.2% Tween20 in PBS (PBS-T) for 1 h at room temperature, reacted overnight at 4°C with either rabbit polyclonal anti-pIRAK1 (Abcam) or β-actin (BD Biosciences) as a control, washed with 0.2% PBS-T, reacted with secondary antibody horseradish peroxidase-conjugated anti-rabbit IgG and anti-mouse IgG (RD, Minneapolis, MN, USA) for 1 h, and washed with PBS-T. After reaction with horseradish peroxidase-conjugated anti-rabbit and anti-mouse IgG, immune complexes were visualized by Super Signal West Pico Chemoluminescent Substrate (Thermo Scientific) according to the manufacturer's suggested procedure. pIRAK1 was analyzed by Image J software under the area, which compensated for β-actin.

Statistical analysis

The results are expressed as mean ± standard error, with the two groups being analyzed by Student's *t*-test and datasets involving more than two groups being analyzed by analysis of variance (ANOVA). *P*-values of <0.05 were considered statistically significant.

Gut sterilization

Mice were treated with ampicillin (1 g/L; Sigma-Aldrich, St. Louis, MO, USA), neomycin (1 g/L; Sigma), metronidazole (1 g/L; Sigma), and vancomycin (500 mg/L; Sigma) in drinking water for 8 weeks.[24] This treatment was followed by feeding with HFD for further 8 weeks.

RESULTS

Fatty liver in HFD-fed mice

AT 16 WEEKS, body weight and serum ALT levels were significantly higher in the HFD-fed mice (group F) than in those fed the control diet (group C) (body weight: C, 41.6 g; F, 51.0 g; serum ALT: C, 34 IU/L; F, 180 IU/L; Fig. 1a,b). Histopathological liver findings from group F demonstrated the absence of fat droplets at 4 weeks (Fig. 1c). However, the deposition of micronodular fat droplets in the centrilobular zone (Fig. 1d) was observed at 8 weeks and macronodular fat droplets and ballooning degeneration (Fig. 1e) were observed at 16 weeks, without any obvious infiltration of inflammatory cells. F4/80 staining for macrophage markers did not demonstrate an increased number of Kupffer cells (Fig. 1f,g).

Upregulation of cytokines in the fatty liver of HFD-fed mice

Histopathological examination of livers from group F demonstrated no obvious infiltration of inflammatory cells, while mRNA levels of the inflammatory cytokines IL-1β and TNF were significantly higher at 16 weeks (Fig. 2a,b).

Upregulation of TLRs in the fatty liver of HFD-fed mice

To confirm whether TLRs expression contributes to the induction of the abovementioned cytokines, we analyzed the mRNA of TLR2, TLR4, TLR5, and TLR9 that recognize bacterial components in the liver. The expression of these TLRs in the liver was not different between the two groups at 4 and 8 weeks, but at 16 weeks, this was significantly higher in the F group than in the C group (Fig. 2c–f). Western blot analysis also demonstrated that the expression of pIRAK1 in the liver was significantly upregulated in the F group compared with that in the C group at 16 weeks (Fig. 2g). These findings suggest that TLR upregulation contributes to the induction of cytokines and that the TLR signal pathway is genetically enhanced in simple steatosis in the absence of inflammation.

Downregulation of TLRs and cytokines in the small intestine of HFD-fed mice

The expression of TLRs that recognize bacterial components was significantly upregulated in the NAFLD liver. Because liver injury has a connection with exposure to bacterial components of intestinal origin, we then examined the small intestine of the NAFLD model mice. The mRNA expression of small intestinal TLR2, TLR4, TLR5, and TLR9 was not significantly different between the two groups at 4 and 8 weeks. Histopathological examination of the small intestine revealed no difference between the groups at 16 weeks, but, mRNA expression of all four TLRs was significantly lower in the F group than in the C group at 16 weeks (Fig. 3a–d). Expression of IL-1β and TNF was also downregulated at 16 weeks (Fig. 3e,f). Moreover, pIRAK1 expression was also significantly decreased in the F group compared with that in the C group at 16 weeks (Fig. 3g). These findings indicate that the TLR signal pathway is genetically attenuated in the NAFLD small intestine.

Antibiotic treatment improved steatosis and TLRs expression in the liver of HFD-fed mice

Small intestinal bacterial overgrowth (SIBO) was reported to coexist with NASH,[14,25] and the following factors can predispose to SIBO: morbid obesity,[26] aging,[27] concurrent use of proton pump inhibitors,[28] and abnormal small intestinal motility.[29] Therefore, we hypothesized that attenuation of TLR signal

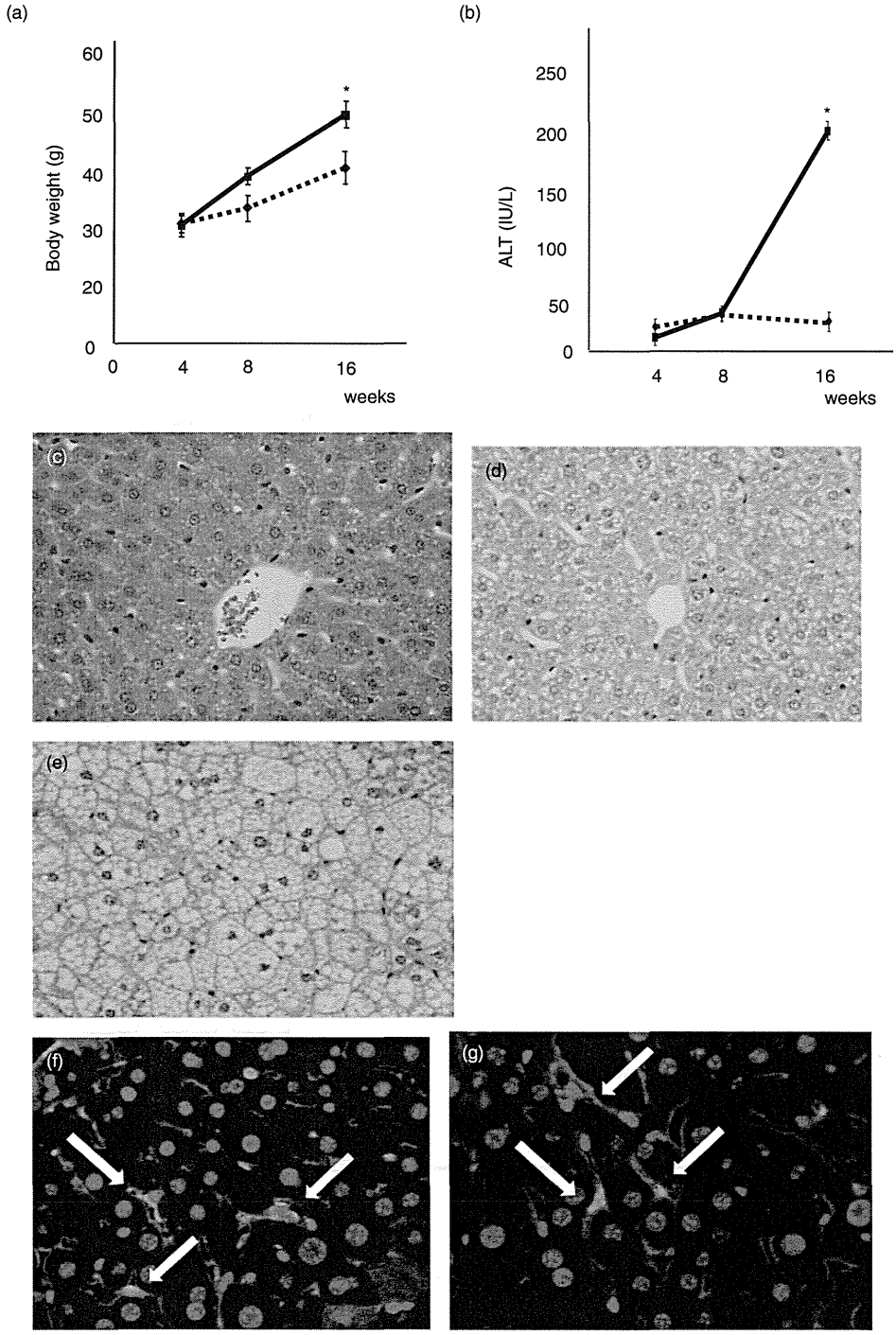

Figure 1 Body weight, serum alanine aminotransferase (ALT), and histopathological findings in high fat diet (HFD)-fed and control mice. Body weight (a) and serum ALT levels (b) were significantly higher in HFD-fed mice (F) than in controls at 16 weeks. Histopathological liver findings in F mice at 4, 8, and 16 weeks with H&E staining (×400, 4 weeks [c]; 8 weeks [d]; 16 weeks [e]). Micronodular fat droplets deposited in hepatocytes in the centrilobular zone at 8 weeks (d). Macronodular fat droplets and ballooning degeneration were marked at 16 weeks, but no obvious infiltration of inflammatory cells was observed (e). F4/80 staining for macrophage marker did not demonstrate any increase in Kupffer cells (control (f); 16 weeks (g); white arrows indicate Kupffer cells, × 400). (*$P < 0.05$).

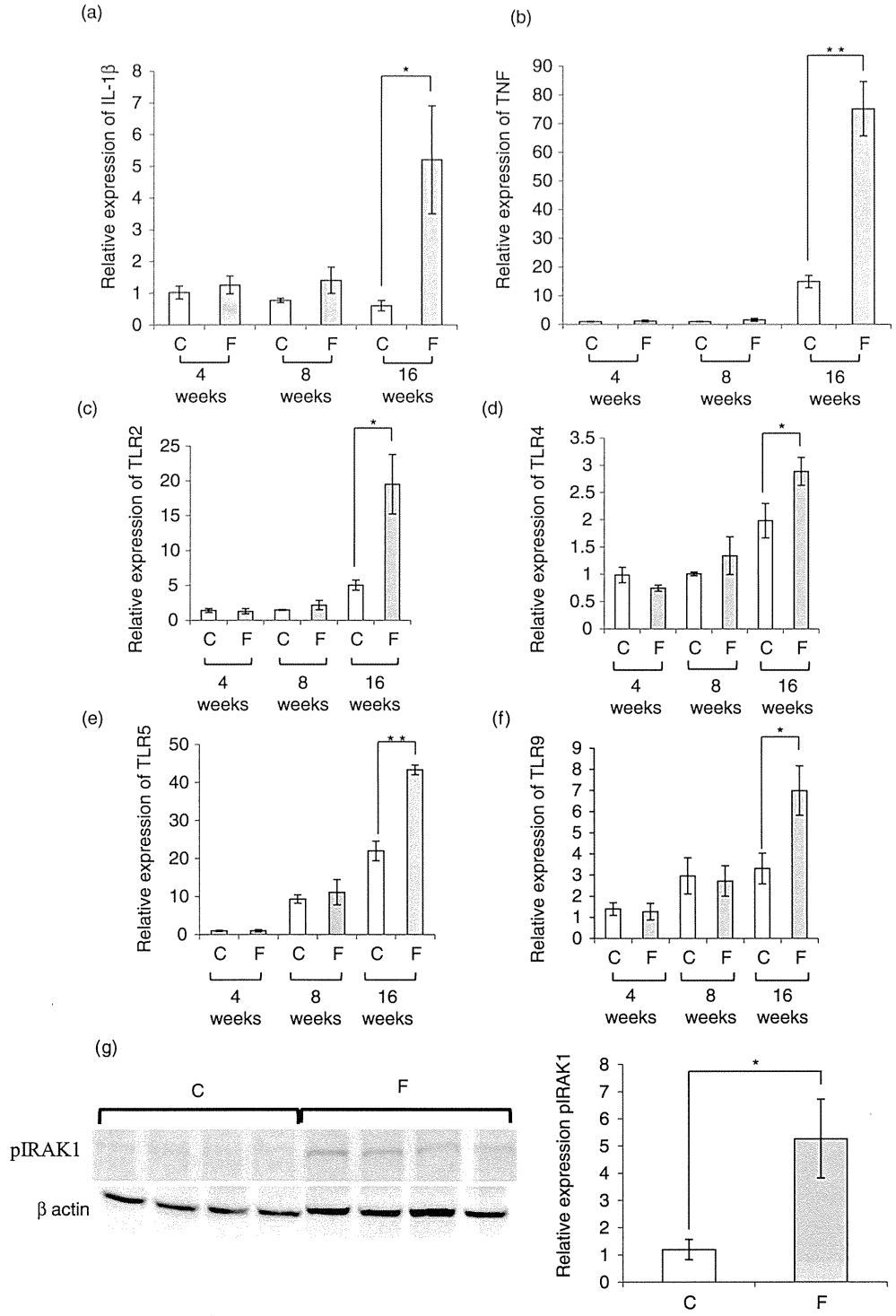

Figure 2 mRNA expression of inflammatory cytokines and Toll-like receptors in the liver of high fat diet (HFD)-fed and control mice. mRNA expression of interleukin (IL)-1β (a), and tumor necrosis factor (TNF) (b) was significantly higher in the liver of HFD-fed mice (F) than in that of controls (C) at 16 weeks. The expression of TLR2 (c), TLR4 (d), TLR5 (e), and TLR9 (f) mRNA was significantly higher in the liver in group F than in group C at 16 weeks. Western blot analysis demonstrated a higher expression of pIRAK1 in the liver in group F than in group C at 16 weeks (g). (*$P < 0.05$, **$P < 0.01$).

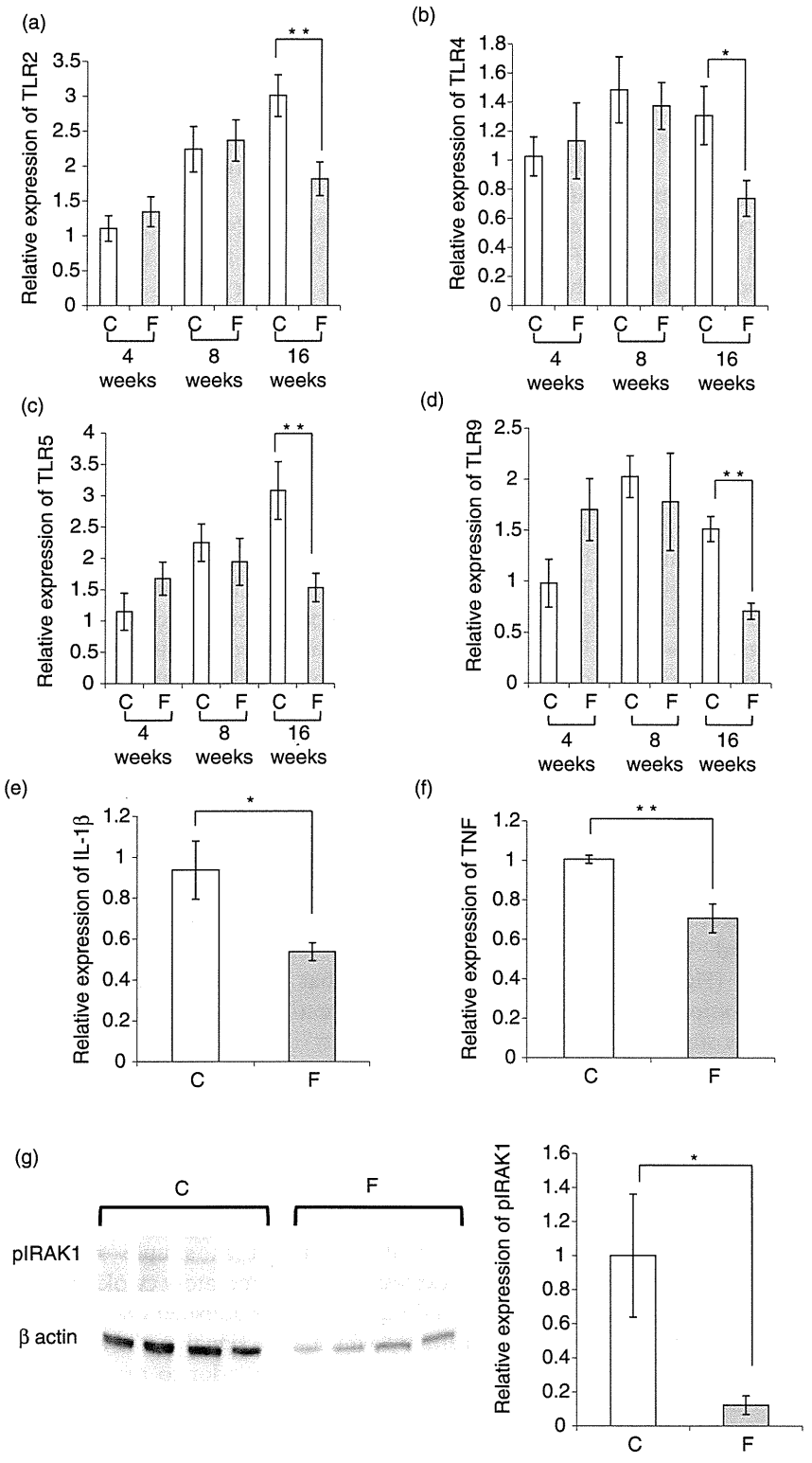

Figure 3 mRNA expression of inflammatory cytokines and Toll-like receptors in the small intestine of high fat diet (HFD)-fed and control mice. mRNA expression of TLR2 (a), TLR4 (b), TLR5 (c), and TLR9 (d) in the small intestine was significantly lower in HFD-fed mice (F) than in control mice (C) at 16 weeks. mRNA expression of IL-1β (e) and TNF (f) in the small intestine was also lower in group F than in group C at 16 weeks. Western blot analysis demonstrated a lower expression of phospho-interleukin-1 receptor-associated kinase1 (pIRAK) in the small intestine in group F than in group C at 16 weeks (g). (*$P < 0.05$, **$P < 0.01$).

pathways may induce immunotolerance, altered levels of microbiota, and bacterial overgrowth in the NAFLD small intestine. To investigate whether intestinal microbiota contribute to TLR expression, we eliminated them by treatment with non-absorbable broad-spectrum antibiotics.[24]

Body weight, serum ALT levels, and serum free fatty acids levels were significantly decreased in mice fed HFD and administered antibiotics (FA) compared with that in the mice fed HFD and water only (FC) (body weight: control diet and water only (CC), 28.9 g; control diet and antibiotics (CA), 28.6 g; FA, 34.7 g; FC, 51.9 g; serum ALT: CC, 19.5 IU/L; CA, 23.4 IU/L; FA, 34.7 IU/L; FC, 147.6 IU/L; serum free fatty acids: CC, 677.1 μEq/L; CA, 818.7 μEq/L; FA, 635.6 μEq/L; FC, 962.7 μEq/L; Fig. 4a–c). Histopathological findings from the livers of FC mice demonstrated the deposition of macronodular fat droplets in the centrilobular area and ballooning degeneration of hepatocytes. In contrast, FA mice showed a marked decrease in steatosis compared with the FC mice (Fig. 4d–g). The expression of TLRs (Fig. 5a–d) and inflammatory cytokines (Fig. 5e,f) was also significantly lower in the liver of FA mice than in that of FC mice. These data indicate associations among intestinal microbiota, TLR expression, and fatty acid metabolism.

Antibiotic treatment did not alter TLRs expression in the small intestine of HFD-fed mice

In the small intestine of mice fed the control diet, the expression of TLR2, TLR4, TLR5, and TLR9 was downregulated by antibiotic treatment (Fig. 6). However, contrary to expectations, the expression in HFD-fed mice did not alter (Fig. 6). These data suggest that microbiota contribute to TLRs expression in the small intestine of mice fed the control diet but not in that of mice fed HFD.

PA upregulated TLR2, TLR4, TLR5, and TLR9 expression in primary Kupffer cells

Because both serum free fatty acids and TLR expression were coincidentally suppressed in the intestinal bacterial eradication model, we examined whether fatty acids would alter TLR expression. First, we investigated TLR expression in primary Kupffer cells.

To determine the effects of fatty acids on TLR expression in Kupffer cells, PA was added to primary Kupffer cells for 24 h, where it induced the deposition of fat droplets (Fig. 7a,b). The mRNA expression of TLR2, TLR4, TLR5, and TLR9 was significantly higher in primary Kupffer cells treated with 10 μM PA for 24 h than in control cells (Fig. 7c).

Immunocytochemistry demonstrated that the expression of pIRAK1 was strongly positive in primary Kupffer cells with fat deposits (Fig. 7d). mRNA expression in IL-1β was not significantly different, but the expression of TNF was significantly higher in primary Kupffer cells exposed to 10 μM PA for 24 h than in controls (Fig. 7e,f). These findings indicate that PA may enhance the TLR signal pathway in Kupffer cells.

PA upregulated TLR4 and TLR9 expression in primary hepatocytes

Second, we examined TLR expression in primary hepatocytes treated with 100 μM PA for 24 h, which induced the deposition of fat droplets in these cells (Fig. 8a,b). mRNA expression of TLR4 and TLR9, but not that of TLR2 and TLR5 was significantly upregulated in primary hepatocytes treated with 100 μM PA for 24 h (Fig. 8c). The expression of IL-1β and TNF was significantly upregulated in primary hepatocytes treated with 100 μM PA for 24 h (Fig. 8d,e). These findings suggest that PA can, at least in part, enhance TLR signal pathways in hepatocytes.

DISCUSSION

MICE FED THE MCD diet demonstrated steatosis, macrophages accumulation, and clustering of neutrophils in the liver. Consequently, the expression of TLR4 and TNF-α was increased; however, the destruction of Kupffer cells prevented an increase in TLR4 expression,[10] indicating that increased expression levels had contributed to infiltration of inflammatory cells. It was reported that fatty liver in NASH resulted in increased liver injury and inflammation following intraperitoneal LPS injection in an MCD diet-induced NASH mouse model, suggesting that the MCD diet-induced NASH liver is sensitive to the TLR4 ligand LPS.[6] In our present model, mice fed HFD for 16 weeks developed steatosis with no histological evidence of inflammation and fibrosis, which is known as simple steatosis. However, the expression of inflammatory cytokines was upregulated, and our findings established that this was the mechanism by which TLR signal pathways were upregulated in the NAFLD liver prior to the development of steatohepatitis. Moreover, F4/80 staining revealed that this upregulation was not affected by an altered number of Kupffer cells but by changes in their activity in regard to inflammatory cytokine production. Our findings show that simple steatosis prior to NASH

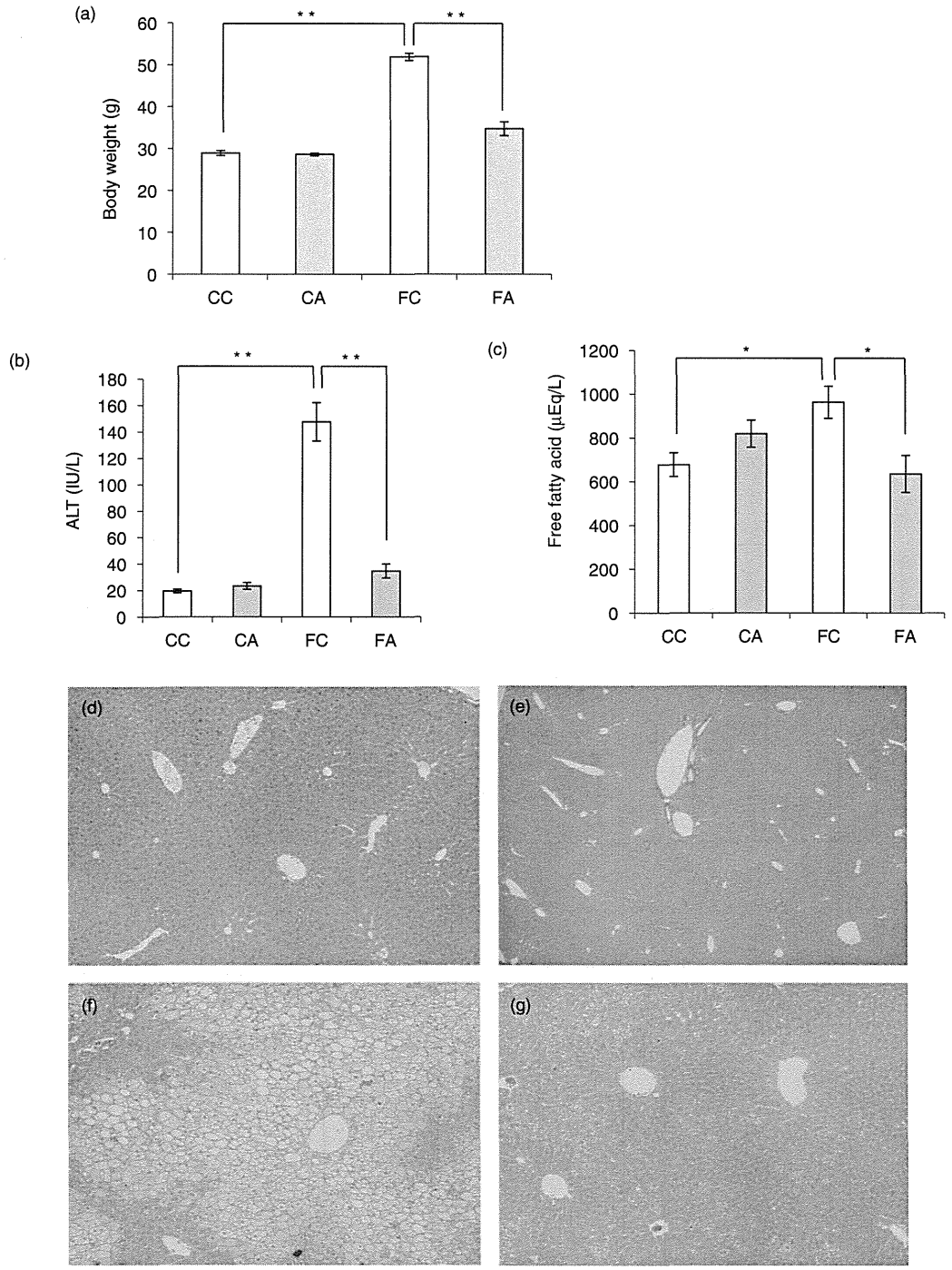

Figure 4 Body weight, serum alanine aminotransferase (ALT) levels, serum free fatty acids, and histopathological findings in high fat diet (HFD)-fed and control mice with or without antibiotic administration. CC, control diet and water only; CA, control diet and antibiotics; FC, HFD and water only; FA, HFD and antibiotics. Body weight was significantly higher in FC mice than in FA mice (a). Serum ALT levels (b) and serum free fatty acids levels (c) were also suppressed in FA mice compared with those in FC mice. Histopathological liver findings for CC (d), CA (e), FC (f), and FA (g) mice with H&E staining (×100) demonstrated macronodular fat droplets and ballooning degeneration in the liver in FC mice, whereas steatosis was obviously suppressed in FA mice. (*$P < 0.05$, **$P < 0.01$).

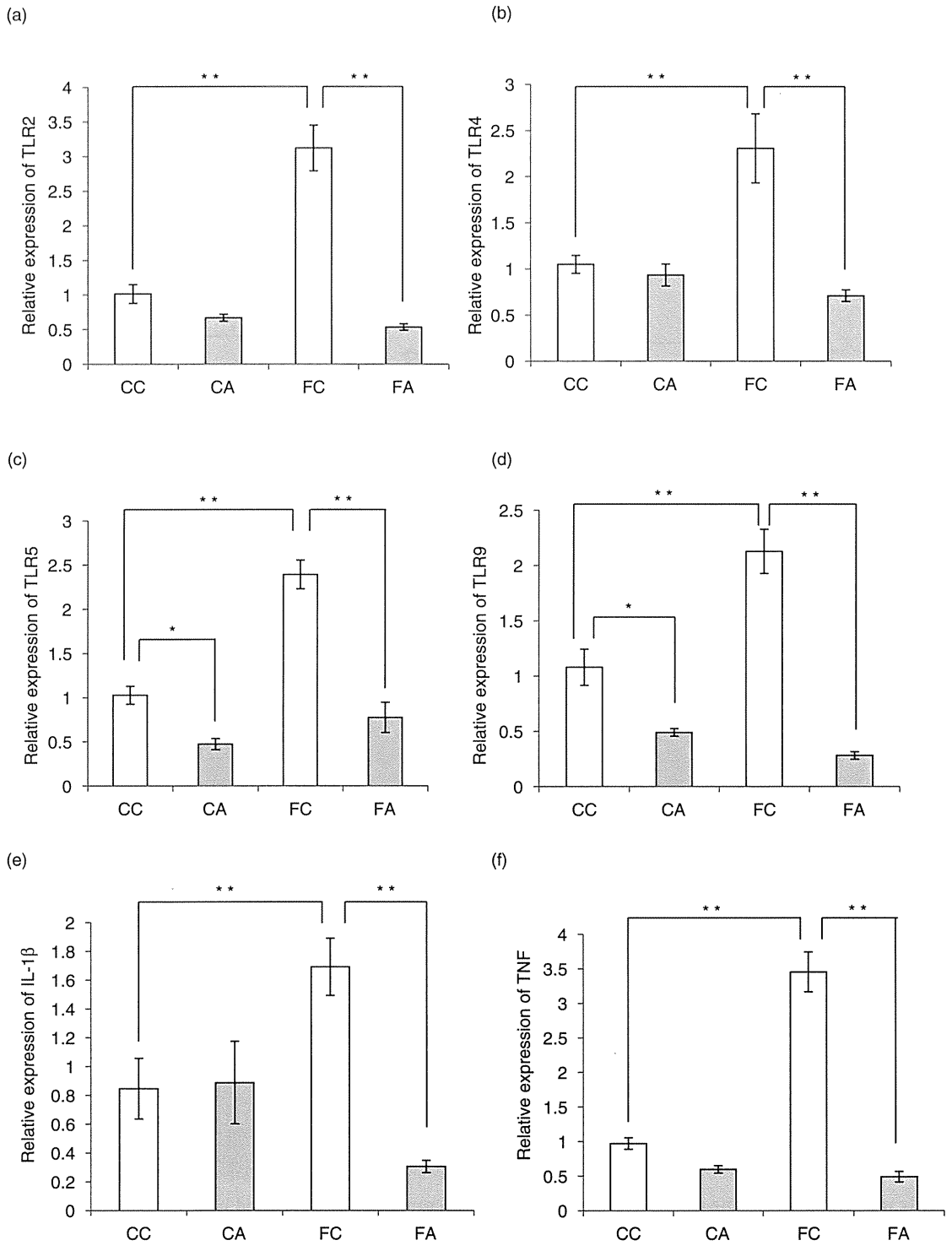

Figure 5 mRNA expression of Toll-like receptors and inflammatory cytokines in the liver in high fat diet (HFD)-fed and control mice with or without antibiotic administration. Expression of TLR2 (a), TLR4 (b), TLR5 (c), and TL9 (d) was suppressed more in the liver of FA mice than in the liver of FC mice. Expression of IL-1β (e) and tumor necrosis factor (TNF) (f) was also suppressed. (*$P < 0.05$, **$P < 0.01$).

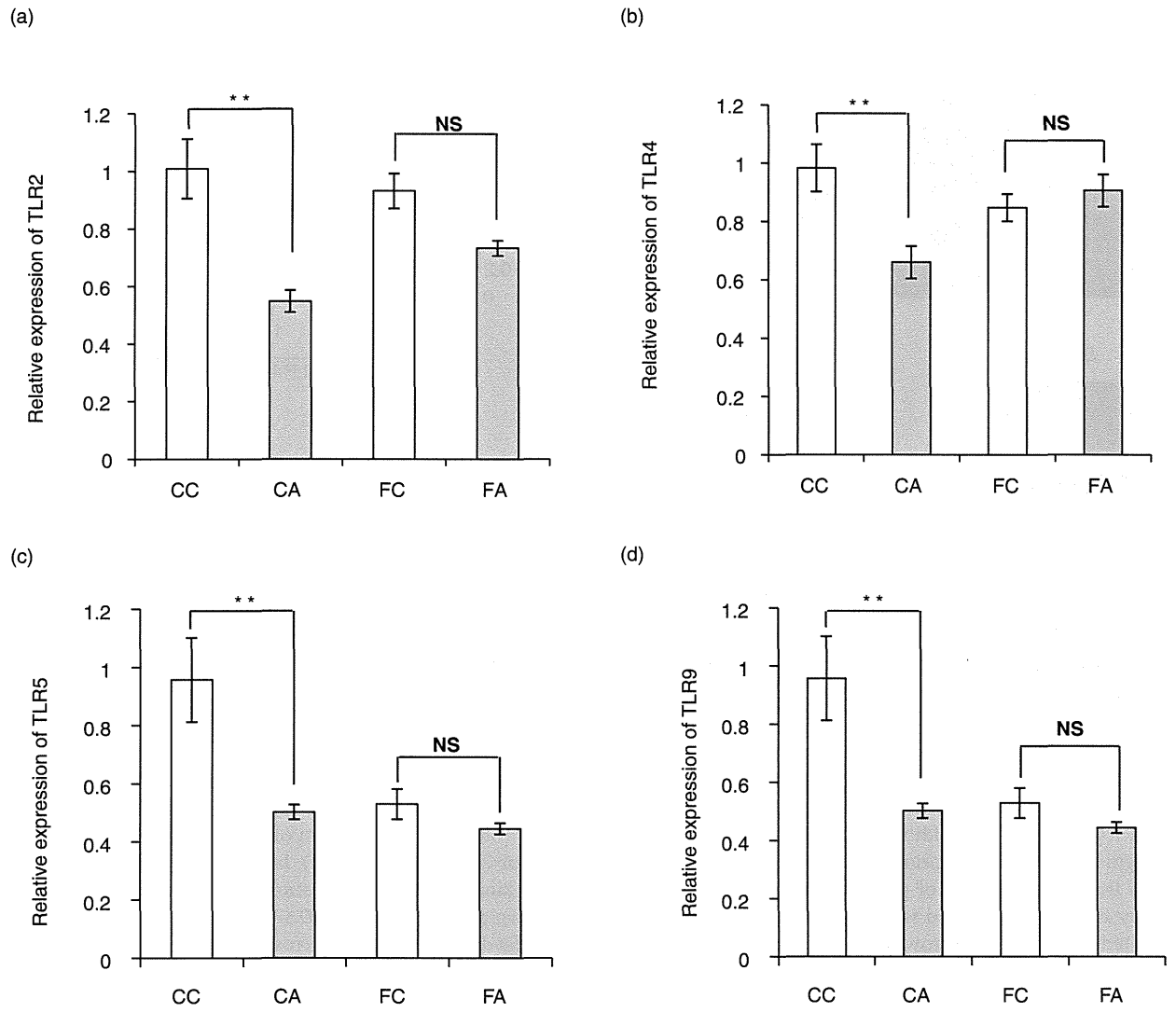

Figure 6 mRNA expression of Toll-like receptors in the small intestine of high fat diet (HFD)-fed and control mice with or without antibiotic administration. Toll-like receptors (TLRs) expression was not altered by antibiotic treatment in non-alcoholic fatty liver disease (NAFLD) small intestine (TLR2 (a), TLR4 (b), TLR5 (c), and TLR9 (d)). (*$P < 0.05$, **$P < 0.01$) (NS, not significant).

demonstrates upregulation of TLR signal pathways and may be more sensitive to the ligands of intestinal microbial components. Bertola *et al.* reported that the expression of TLRs and certain cytokines/chemokines in genes was upregulated in biopsy specimens of morbidly obese patients with histologically normal liver or severe steatosis with or without NASH,[30] and our findings from this animal study concur with this.

Although many studies have examined the association between TLR signal pathways and the pathogenesis of NASH, these reports focused mainly on hepatocytes, Kupffer cells, and hepatic stellate cells.[6,10,12,31] However, small intestinal microbiota are the cause of liver damage in NASH, and to our knowledge, this is the first report to investigate the expression of intestinal TLR signal pathways in NAFLD model and to reveal a discrepancy in TLRs expression in the gut-liver axis. The microbial TLR signal pathway and downstream cytokines were downregulated in the small intestine of NAFLD model and this downregulation may contribute to imbalance of the immune system and, consequently, alter the microflora component ratio and induce SIBO with NAFLD.

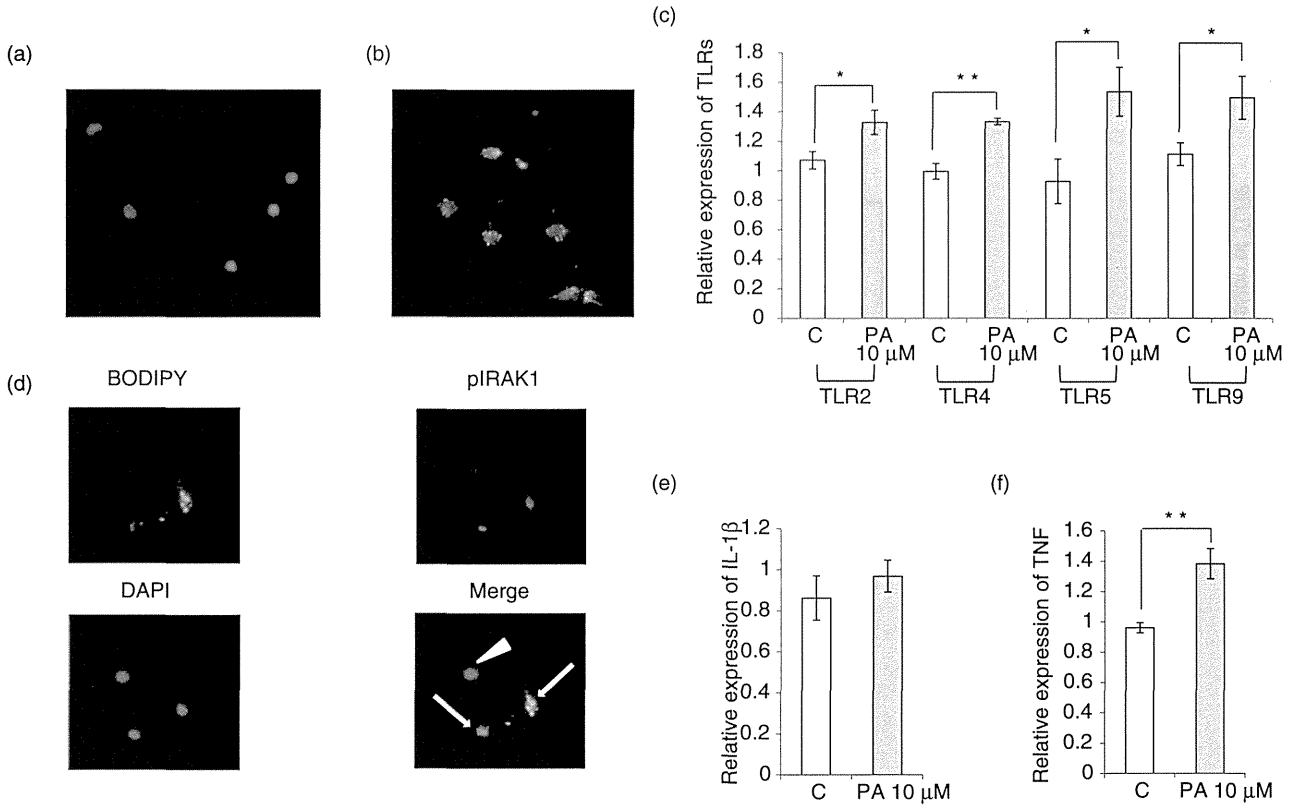

Figure 7 mRNA expression of Toll-like receptors and inflammatory cytokines in primary Kupffer cells treated with palmitic acid (PA). Treatment by PA for 24 h induced deposition of fat droplets in primary Kupffer cells (a: control, b: treatment with 10 μM PA, BODIPY (green), 4′6′-diamidino-2-phenylindole dihydrochloride (DAPI) [blue]). The expression of TLR2, TLR4, TLR5, and TLR9 was significantly higher in primary Kupffer cells treated with 10 μM PA for 24 h (C: control) (c). Immunocytochemistry demonstrated that the expression of phospho-interleukin-1 receptor-associated kinase1 (pIRAK) was strongly positive in fat deposited primary Kupffer cells treated with 10 μM PA for 24 h (d: BODIPY (green), pIRAK1 (red) and DAPI (blue). Arrow: Kupffer cells deposited in fat droplets. Arrow head: Kupffer cell deposited in absence of fat droplets). Tumor necrosis factor (TNF) expression was significantly higher in primary Kupffer cells treated with 10 μM PA for 24 h (IL-1β (e), TNF (f)) ($^{*}P < 0.05$, $^{**}P < 0.01$).

We used a mouse model gut-sterilized with antibiotics to confirm whether there is an association between gut microbiota and TLR expression in NAFLD. In our model, oral caloric intake was not significantly different between FA and FC mice, but, body weight, serum ALT levels, and serum free fatty acids levels were significantly suppressed in the FA mice. Furthermore, histopathological findings showed a marked decrease in steatosis in this group. Interestingly, the expression of TLRs and downstream cytokines was suppressed in FA mice compared with that in FC mice. In contrast, in an ethyl alcohol-induced liver injury model, liver TLR expression was found to be independent of gut microbiota despite a decrease in fatty liver and liver injury by antibiotic administration.[9] Our findings suggest that, directly or indirectly, gut microbiota contribute to TLR expression in the liver of the NAFLD model. Because antibiotics administration also decreased serum free fatty acids in FA mice, we focused on the association between fatty acid metabolism and gut microbiota. There are three reasons for the suppression of serum free fatty acids in FA mice. The first is a decrease in adipocytes accompanied by suppression of increasing body weight. This may be explained by the fact that obesity-associated microbiota, which increase the capacity to harvest energy from the diet, were eradicated by antibiotics.[13] We investigated 16 s rRNA based analysis of fecal microbiota by the terminal restriction fragment length polymorphism method and confirmed alteration in fecal microbiota of FA mice compared with that of FC

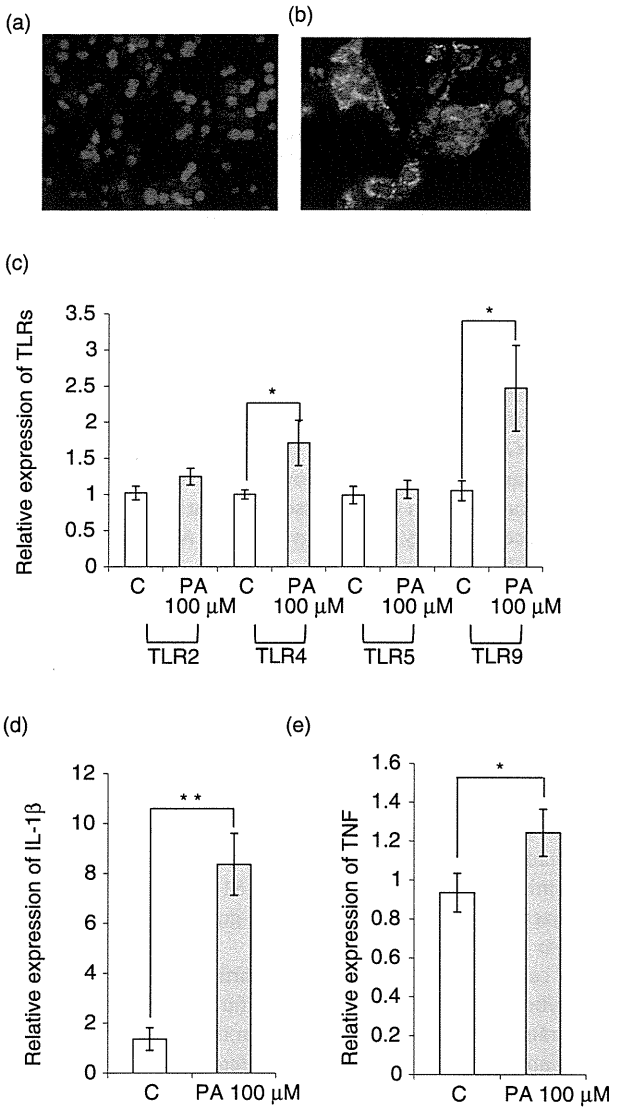

Figure 8 mRNA expression of Toll-like receptors and inflammatory cytokines in primary hetatocytes treated with palmitic acid (PA). Treatment by PA for 24 h induced the deposition of fat droplets in primary hepatocytes (a: control, b: treatment with 100 μM PA, BODIPY (green), 4′6′-diamidino-2-phenylindole dihydrochloride (DAPI) [blue]). The expression of TLR4 and TLR9 mRNA was significantly upregulated in primary hepatocytes treated with 100 μM PA for 24 h (C: control) (c). The expression of tumor necrosis factor (TNF) and interleukin (IL)-1β was significantly higher in primary hepatocytes treated with 100 μM PA for 24 h (IL-1β (d), TNF [e]) (*$P < 0.05$, **$P < 0.01$).

mice (data not shown). The second reason is a decrease in the release of free fatty acids from adipocytes. In obese individuals, it has been reported that gut microbiota can suppress the expression of fasting-induced adipose factor (Fiaf), which increases the activity of lipoprotein lipase, leading to the production of triglyceride storage in adipocytes and an increased supply of fatty acids.[32] The expression of intestinal Fiaf was significantly upregulated in FA mice compared with FC mice in our experiment (data not shown), indicating that gut-sterilization may contribute to a reduction in the release of serum free fatty acids from adipocytes through increased intestinal Fiaf expression. The third reason is a decrease in *de novo* liver lipogenesis. It is reported that microbiota can increase hepatic lipogenesis through the expression of sterol response element binding protein 1 (SREBP1) and carbohydrate response element binding protein (ChREBP).[33] The expression of both SREBP1 and ChREBP was significantly suppressed in FA mice compared with that in FC mice in our experiment (data not shown), indicating that the suppression of serum free fatty acids, at least in part, contributes to a decrease in hepatic *de novo* lipogenesis through the suppression of both SREBP1 and ChREBP. Our findings suggest both alteration in microflora and a decrease in *de novo* lipogenesis in the liver of the gut-sterilized model, but it is unknown whether the release of free fatty acids from adipocytes decreases.

Next, we hypothesized that fatty acids could alter TLRs expression in the liver. We showed that the expression of TLR2, TLR4, TLR5, TLR9, and TNF were significantly higher in primary Kupffer cells treated with PA than in control cells, while that of TLR4, TLR9, TNF, and IL-1β was upregulated in primary hepatocytes treated with PA. Although our *in vitro* study suggests that PA directly stimulates the induction of TLRs, others report that saturated fatty acids (SFA) including PA stimulate NFκB promoter activity through the activation of the TLR signal pathway. It is also reported that SFA plays a role as TLR4 ligand.[34,35] Therefore, the induction of downstream cytokines may have contributed to both the upregulation of TLRs and stimulation of TLR4 by PA. These findings suggest that Kupffer cells and hepatocytes are susceptible to bacterial components via upregulation of TLRs by PA in the pro-inflammatory state of NAFLD.

In contrast, although TLRs expression in the small intestine of HFD-fed mice was not altered by antibiotic treatment, it was downregulated in control mice. Therefore, we hypothesized that luminal HFD itself could attenuate TLRs expression in the small intestine. Caco2 cells that are human epithelial cell lines treated with PA or OA showed lower expression of TLR2, TLR5, and TLR9 compared with control cells (data not shown). These data suggest that fatty acids may partly contribute

to the attenuation of TLRs expression in the small intestine.

In conclusion, TLRs expression was downregulated in the NAFLD small intestine, and this may be contributed to an increase in free fatty acids through alteration of gut microbiota. In contrast, the hepatic TLR signal pathway was upregulated and susceptible to microbial components by increased free fatty acids in the pro-inflammatory state of NAFLD. Our findings suggest that discrepancy in TLR signals in the gut-liver axis may be associated with the pathogenesis of progression to NASH through an increase in free fatty acids. Because there is no specific treatment for human NASH, early intervention in the pro-inflammatory state may be important for the prevention of its development from simple steatosis. Because free fatty acids play an important role in the development of the pro-inflammatory state of NAFLD, we consider that both fatty acid metabolism and gut microbiota in the pro-inflammatory state may be useful targets for preventive treatment against NASH development.

ACKNOWLEDGMENTS

THIS WORK WAS supported, in part, by Grants-in-Aid for Young Scientists (B) provided by the Ministry of Education, Culture, Sports, Science, and, Technology, Japan.

REFERENCES

1 Ludwig J, Viggiano TR, McGill DB, Brewer NS. Nonalcoholic steatohepatitis: Mayo Clinic experiences with a hithero unnamed disease. *Mayo Clin Proc* 1980; **55:** 482–8.
2 Lazo M, Clark JM. The epidemiology of nonalcoholic fatty liver disease: a global perspective. *Semin Liver Dis* 2008; **28:** 339–50.
3 Day CP, James OF. Steatohepatitis: a role of two "hit"? *Gastroenterology* 1998; **114:** 842–5.
4 Marra F, Bertolani C. Adipokines in liver disease. *Hepatology* 2009; **50:** 957–62.
5 George DK, Goldwurm S, MacDonald GA *et al.* Increased hepatic iron concentration in nonalcoholic steatohepatitis is associated with increased fibrosis. *Gastroenterology* 1988; **114:** 311–18.
6 Szabo G, Velayudham A, Romics L Jr, Mandrekar P. Modulation of non-alcoholic steatohepatitis by pattern recognition receptors in mice: the role of toll-like receptor 2 and 4. *Alcohol Clin Exp Res* 2005; **29** (11 Suppl): 140S–5S.
7 Seki E, Brenner DA. Toll-like receptors and adaptor molecules in liver disease: update. *Gastroenterology* 2008; **48:** 322–35.
8 Takeda K, Akira S. TLR signaling pathway. *Semin Immunol* 2004; **16:** 3–9.
9 Gustot T, Lemmers A, Moreno C *et al.* Differential liver sensitization to Toll-like receptor pathways in mice with alcoholic fatty liver. *Hepatology* 2006; **43:** 989–1000.
10 Rivera CA, Adegvoyage P, van Rooijen N, Tagalicud A, Allman M, Wallace M. Toll-like receptor-4 signaling and Kupffer cells play pivotal roles in the pathogenesis of non-alcoholic steatohepatitis. *J Hepatol* 2007; **47:** 571–9.
11 Imajo K, Fujita K, Yoneda M *et al.* Hyperresponsivity to low-dose endotoxin during progression to nonalcoholic steatohepatitis is regulated by leptin mediated signaling. *Cell Metab* 2012; **16:** 44–54.
12 Miura K, Kodama Y, Inokuchi S *et al.* Toll-like receptor 9 promotes steatohepatitis by induction of interleukin-1β in mice. *Gastroenterology* 2010; **139:** 323–34.
13 Turnbaugh PJ, Ley RE, Mahowald MA, Magrini V, Mardis ER, Gordon JI. An obesity-associated gut microbiome with increased capacity for energy harvest. *Nature* 2006; **444:** 1027–31.
14 Shanab AA, Scully P, Crosbie O *et al.* Small intestinal bacterial overgrowth in nonalcoholic steatohepatitis: association with toll-like receptor 4 expression and plasma levels of interleukin 8. *Dig Dis Sci* 2011; **56:** 1524–34.
15 Ley RE, Turnbaugh PJ, Klein S, Gordon JI. Human gut microbes associated with obesity. *Nature* 2006; **444:** 1022–3.
16 Cani PD, Bibiloni R, Knauf C *et al.* Changes in gut microbiota control metabolic endotoxemia-induced inflammation in high fat diet induced obesity and diabetes in mice. *Diabetes* 2008; **57:** 1470–81.
17 Bajzer M, Seeley RJ. Obesity and gut flora. *Nature* 2006; **444:** 1009–10.
18 de La Serre CB, Ellis CL, Lee J, Hartman AL, Rutledge JC, Raybould EE. Propensity to high-fat diet-induced obesity in rats is associated with changes in the gut microbiota gut inflammation. *Am J Physiol Gastrointest Liver Physiol* 2010; **299:** G440–8.
19 Vijay-Kumar M, Aitken JD, Carvalho A *et al.* Metabolic syndrome and altered gut microbiota in mice lacking Toll-like receptor 5. *Science* 2010; **328:** 228–31.
20 Santaolalla R, Fukata M, Abreu M. Innate immunity in the small intestine. *Curr Opin Gastroenterol* 2011; **27:** 125–31.
21 Lodes MJ, Cong Y, Elson CO *et al.* Bacterial flagellin is a dominant antigen in Crohn disease. *J Clin Invest* 2004; **113:** 1296–306.
22 Munthe-Kaas AC, Berq T, Seqlen PO, Seljelid R. Mass isolation and culture of rat Kupffer cells. *J Exp Med* 1975; **141:** 1–10.
23 Gottipati S, Rao NL, Fung-Leung WP. IRAK1: a critical signaling mediator of innate immunity. *Cell Signal* 2008; **20:** 269–76.
24 Seki E, Minicis SD, Osterreicher CH *et al.* TLR4 enhances TGF-β signaling and hepatic fibrosis. *Nat Med* 2007; **13:** 1324–32.

25 Wigg AJ, Roberts-Thomson IC, Dymock RB, McCarthy PJ, Grose RH, Cummins AG. The role of small intestinal bacterial overgrowth, intestinal permeability, endotoxaemia, and tumor necrosis factor alpha in the pathogenesis of non-alcoholic steatohepatitis. *Gut* 2001; **48**: 206–11.
26 Sabate JM, Jouet P, Harnois F *et al.* High prevalence of small intestinal bacterial overgrowth with morbid obesity: a contributor to severe hepatic steatosis. *Obes Surg* 2008; **18**: 371–7.
27 Pillotto A, Franceschi M, Del Favero G, Fabrello R, Di Mario F, Valerio G. The effect of aging on oro-cecal transit time in normal subjects and patients with gallstone disease. *Aging (Milano)* 1995; **7**: 234–7.
28 Elphick DA, Chew TS, Higham SE, Bird N, Ahmad A, Sanders DS. Small bacterial overgrowth in symptomatic older people: can it be diagnosed earlier? *Gerontology* 2005; **51**: 396–401.
29 Soza A, Riquelme A, Gonzalez R *et al.* Increased orocecal transit time in patients with nonalcoholic fatty liver disease. *Dig Dis Sci* 2005; **50**: 1136–40.
30 Bertola A, Bonnafous S, Anty R *et al.* Hepatic expression patterns of inflammatory and immune response genes associated with obesity and NASH in morbidly obese patients. *PLoS ONE* 2010; **5**: e13577.
31 Rivera CA, Gaskin LT, Allman M *et al.* Toll-like receptor 2 deficiency enhances non-alcoholic steatohepatitis. *BMC Gastroenterol* 2010; **10**: 52.
32 Backhed F, Ding H, Wang T *et al.* The gut microbiota as an environmental factor that regulates fat storage. *Proc Natl Acad Sci U S A* 2004; **101**: 15718–23.
33 Prakash S, Rodes L, Coussa-Charley M, Duchesneau CT. Gut mictobiota: next frontier in understanding human health and development of biotherapeutics. *Biologics* 2011; **5**: 71–86.
34 Lee JY, Plakidas A, Lee WH *et al.* Differential modulation of Toll-like receptors by fatty acids: preferential inhibition by n-3polyunsaturated fatty acids. *J Lipid Res* 2003; **44**: 909–16.
35 Lee JY, Gao Z, Youn HS *et al.* Reciprocal modulation of Toll-like recptor-4 signaling pathways involving MyD88 and phosphatidylinositol 3-kinase/AKT by saturated and polyunsaturated fatty acids. *J Biol Chem* 2003; **278**: 37041–51.

Int Canc Conf J (2015) 4:41–47
DOI 10.1007/s13691-014-0167-5

CASE REPORT

Effectiveness of pazopanib for postoperative recurrence of granulocyte colony-stimulating factor-producing primary hepatic angiosarcoma

Koji Sawada · Manabu Soma · Shunsuke Nakajima · Takumu Hasebe · Shigeaki Maeda · Masami Abe · Takaaki Ohtake · Yoshinori Saito · Chitomi Hasebe · Masahiro Yamamoto · Mikihiro Fujiya · Yoshihiro Torimoto · Yutaka Kohgo

Received: 18 December 2013 / Accepted: 8 May 2014 / Published online: 3 June 2014

Abstract A 38-year-old Japanese woman was referred to our hospital with complaints of fever, general fatigue, and upper abdominal discomfort. Computed tomography revealed a massive tumor in the right lobe of the liver, and laboratory data demonstrated increased white blood cell (WBC) count and serum granulocyte colony-stimulating factor (G-CSF) level. An extended right hepatectomy was performed, and pathological examination revealed spindle-shape tumor cells that formed vessel-like structures that were compatible with hepatic angiosarcoma. As a rapid recurrence occurred after surgery, S-1 was administered as a first-line chemotherapy, and weekly paclitaxel was administered as the second-line chemotherapy. However, patient eventually became resistant to these therapies. Therefore, pazopanib, a multitargeted tyrosine kinase inhibitor, was administered, after which both the WBC count and G-CSF level rapidly decreased. ^{18}F-fluorodeoxyglucose positron emission tomography (FDG-PET) revealed decreased FDG uptake. This is the first report on the administration of pazopanib as a third-line chemotherapeutic agent for treating G-CSF-producing primary hepatic angiosarcoma. The efficacy of this therapy was demonstrated with FDG-PET.

Keywords Pazopanib · Primary hepatic angiosarcoma · Granulocyte colony-stimulating factor

K. Sawada (✉) · T. Ohtake
Department of Clinical Gastroenterology and Hepatology on Co-operative Network, Asahikawa Medical University, 2-1 Midorigaoka Higashi, Asahikawa 078-8510, Japan
e-mail: k-sawada@asahikawa-med.ac.jp

M. Soma · S. Nakajima · T. Hasebe · S. Maeda · M. Abe · T. Ohtake · M. Fujiya · Y. Kohgo
Division of Gastroenterology and Hematology/Oncology, Department of Medicine, Asahikawa Medical University, Asahikawa, Japan

Y. Saito
Department of Gastroenterology, Asahikawa-Kosei General Hospital, Asahikawa, Japan

C. Hasebe
Department of Gastroenterology, Asahikawa Red Cross Hospital, Asahikawa, Japan

M. Yamamoto
Division of Tumor Pathology, Department of Pathology, Asahikawa Medical University, Asahikawa, Japan

Y. Torimoto
Oncology Center, Asahikawa Medical University Hospital, Asahikawa, Japan

Introduction

Angiosarcoma, which is derived from vascular endothelial cells, commonly arises from the breast, skin, and soft tissues [1]. Primary hepatic angiosarcoma is an extremely rare malignant tumor accounting for 0.1–2 % of all hepatic malignant tumors [2, 3]. The carcinogenesis of angiosarcoma has been reported to involve exposure to vinyl chloride, thorotrast, and arsenic [2]. However, many recent cases without exposure to these factors have been reported, and the cause of angiosarcoma remains unknown.

Pazopanib, a multitargeted tyrosine kinase inhibitor against vascular endothelial growth factor receptor (VEGFR) and platelet derived growth factor receptor (PDGFR), was reported to significantly increase progression-free survival in a phase-III trial of patients with advanced soft tissue sarcoma after the failure of a standard chemotherapy [4]. The phase-III trial of pazopanib included patients with most soft tissue sarcoma subtypes, the majority of whom

were diagnosed with leiomyosarcoma and synovial sarcoma; only three had soft tissue angiosarcoma, and there were no cases of hepatic angiosarcoma. As angiosarcoma is derived from VEGFR-positive and PDGFR-positive vascular endothelial cells [5], it is worthwhile to treat hepatic angiosarcoma by pazopanib after the failure of a standard chemotherapy.

We herein report a case of primary hepatic angiosarcoma that rapidly recurred after extended hepatectomy and conventional chemotherapies. After the failure of the second-line chemotherapy, pazopanib was administered as the third-line chemotherapy. ^{18}F-fluorodeoxyglucose positron emission tomography (FDG-PET) revealed decreased FDG uptake by the tumor. To the best of our knowledge, this is the first report on the administration of pazopanib as the third-line chemotherapeutic agent for treating granulocyte colony-stimulating factor (G-CSF)-producing primary hepatic angiosarcoma. The efficacy of this therapy was evaluated with FDG-PET.

Case

A 38-year-old woman was referred to our hospital with complaints of fever, general fatigue, and upper abdominal discomfort. She had no history of exposure to vinyl chloride, thorotrast, or arsenic. A physical examination revealed hepatomegaly and mild tenderness in the right upper quadrant. Laboratory data demonstrated an increased white blood cell (WBC) count with neutrophil dominance and increased levels of alkaline phosphatase, γ-glutamyl transpeptidase, and C-reactive protein (CRP) (Table 1). Increased serum transaminase level and decreased hepatic reserve function were not observed (Table 1). Computed tomography (CT) revealed a massive tumor in the right lobe of the liver (Fig. 1a, b); however, all common tumor markers were within the normal range. Because severe inflammation, including bacterial infection, was not observed, the cause of the patient's leukocytosis and increased CRP level was investigated by bone marrow aspiration. The pathological findings did not detect bone marrow proliferative disease. Further analysis revealed that the increased number of neutrophils was due to a high level of serum G-CSF (368 pg/mL; normal range 0.0–39.0 pg/mL). A liver biopsy was performed, and the tumor was diagnosed as suspected poorly differentiated cholangiocellular carcinoma. Because FDG-PET did not indicate intrahepatic or distant metastasis (Fig. 1c), an extended right hepatectomy was performed after preoperative portal vein embolization. The pathological findings of the surgical specimens showed spindle-shape tumor cells that formed vessel-like structures. Immunohistochemical staining was positive for vimentin and weakly positive for both factor VIII-related antigen and CD31, which suggested hepatic angiosarcoma. Moreover, immunohistochemical staining was also positive for G-CSF (Calbiochem) in tumor cells (Fig. 2a–e). One month after the hepatectomy, CT revealed a rapid recurrence of the tumor in the left adrenal gland and pancreas (Fig. 3). S-1 (100 mg/day) was administered as a first-line chemotherapy. However, 1 month later, CT and FDG-PET indicated the growth of angiosarcoma in the left adrenal gland, pancreas, bilateral lungs, left breast, liver, peritoneum, left thyroid lobe, and left wrist joint (Fig. 4a–c). Weekly paclitaxel (PTX, 130 mg/week) was administered as the second-line chemotherapy [6], and after the first course of weekly PTX, FDG-PET revealed decreased FDG uptake in most metastatic lesions (Fig. 4d). The standardized uptake values (SUVs) of the left adrenal gland (12.6), pancreas (7.8), right lung (5.7), liver (7.5), peritoneum (8.9), and left thyroid lobe (7.4) decreased to 4.8, 7.4, 1.2, 6.8, 1.5, and 2.6, respectively. The WBC count and G-CSF level also improved (Fig. 5). However, after two PTX further courses, FDG-PET revealed an increased in FDG uptake in all previous lesions and the appearance of new lesions including skin in the lower abdomen as well as the lymph nodes in the abdomen, mediastinum, and neck (Fig. 6a). The patient's WBC count and G-CSF level gradually increased (Fig. 5). Immunohistochemical staining was negative for VEGFR2 (Cell Signaling Technology), but positive for PDGFRβ (Santa Cruz) in tumor cells (Fig. 7). Therefore, after obtaining informed consent from the patient and her family and after the consensus of the cancer board, including other department doctors, pazopanib (800 mg/day) was administered as the third-line chemotherapy. After 7 days, her WBC count rapidly decreased. After 9 days, radiation therapy (8 Gy per fraction) was performed because of persistent pain in her left wrist. Three weeks after the initial pazopanib administration, the patient's WBC count increased to 31,450/μL, but the G-CSF level decreased (Fig. 5). Moreover, FDG-PET indicated decreased FDG uptake in most of the lesions. The SUVs of the left adrenal gland (10.8), pancreas (9.9), right lung (4.5), liver (9.3), peritoneum (7.7), left thyroid lobe (12.5), skin in the lower abdomen (9.6), and lymph nodes in the mediastinum (7.1) decreased to 6.4, 5.7, 3.1, 3.6, 3.2, 11.6, 4.6, and 4.4, respectively. These findings suggested that an increased WBC count is accompanied by tumor necrosis, and pazopanib is an effective therapy for advanced hepatic angiosarcoma (Figs. 5, 6b). However 1 month after the pazopanib administration, the patient vomited blood because of a hemorrhagic gastric ulcer; thereafter, her platelet count decreased (0.7×10^4/μL), and the levels of total bilirubin, alanine aminotransferase, fibrin degradation products, and CRP increased (14.4 mg/dL, 1,642 U/L, 86.6 μg/mL, and 20.13 mg/dL, respectively), which indicated disseminated intravascular coagulation

Table 1 Laboratory data

WBC	25,200/μL	T.P.	7.6 g/dL	Na	143 mEq/L
Nuet	93.0 %	Alb	3.7 g/dL	K	3.9 mEq/L
Lymp	6.0 %	T.Bil	0.3 mg/dL	Cl	105 mEq/L
Mono	1.0 %	D.Bil	0.1 mg/dL	CRP	4.37 ng/mL
RBC	4.15×10^6/μL	ALT	22 IU/L		
Hb	11.6 g/dL	AST	15 IU/L	AFP	4.1 ng/mL
Ht	35.0 %	ALP	870 IU/L	PIVKA-II	18 mAU/ML
PLT	30.9×10^4/μL	LDH	378 IU/L	CA19-9	0.6 ng/mL
		γGTP	165 IU/L	CEA	15 U/mL
		ChE	239 IU/L		
PT %	85.1 %	BUN	7.6 mg/dL	HBs-Ag (−)	
PT-INR	1.14	Cr	0.44 mg/dL	HCV-Ab (−)	
				G-CSF	368 pg/mL

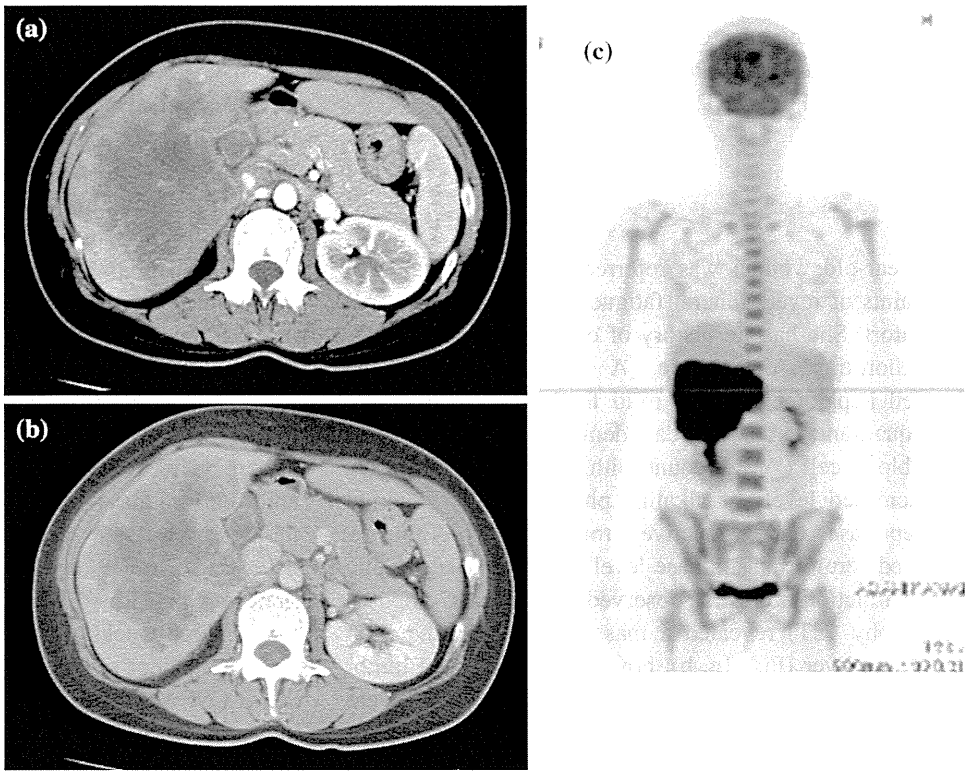

Fig. 1 **a, b** Computed tomography revealed a massive heterogeneous tumor in the right lobe of the liver. Dynamic studies showed slight peripheral enhancement in the arterial phase (**a**) and prolonged enhancement in the delayed phase (**b**). **c** FDG-PET demonstrated strong accumulation in the liver

(DIC) and hepatic failure. Despite the discontinuation of pazopanib and intensive therapy for DIC, the patient eventually died 1 month later because of multiple organ failure and acute pneumonia. An autopsy revealed mild necrosis of hepatic angiosarcoma, suggesting a partial response to pazopanib.

Discussion

We herein report the first case demonstrating the efficacy of pazopanib administration as a third-line chemotherapy for treating G-CSF-producing primary hepatic angiosarcoma, which was confirmed by FDG-PET. Angiosarcoma appears to account for only 2 % of all sarcomas [7]. Primary hepatic angiosarcoma is extremely rare, representing only 4 % of all angiosarcomas [1], and there are no reports describing G-CSF-producing hepatic angiosarcoma. Clinical presentation of angiosarcoma shows an aggressive behavior. The median survival is only 6 months without any therapy, and most patients die within 1 year after the diagnosis [8].

When the lesion is confined to one lobe of the liver without any metastases, hepatectomy has proven to be